

Computational Fluid Dynamics Simulation of Gas-Liquid Phase Stirred Tank

Thiyam Tamphasana Devi, Bimlesh Kumar

Abstract—A Computational Fluid Dynamics (CFD) technique has been applied to simulate the gas-liquid phase in double stirred tank of Rushton impeller. Eulerian-Eulerian model was adopted to simulate the multiphase with standard correlation of Schiller and Naumann for drag co-efficient. The turbulence was modeled by using standard k-ε turbulence model. The present CFD model predicts flow pattern, local gas hold-up, and local specific area. It also predicts local kLa (mass transfer rate) for single impeller. The predicted results were compared with experimental and CFD results of published literature. The predicted results are slightly over predicted with the experimental results; however, it is in reasonable agreement with other simulated results of published literature.

Keywords—Eulerian-Eulerian, gas-hold up, gas-liquid phase, local mass transfer rate, local specific area, Rushton Impeller.

I. INTRODUCTION

GAS-LIQUID vessels are widely used in several process industries to carry out various gas-liquid reactions. The characteristic of fluid dynamics in gas-liquid phases is generally understood through the mechanism of interaction between these two phases in terms of gas hold up, interfacial specific area and mass transfer. Studies based on gas-liquid phase in stirred tank were done by several researchers like [1]-[7]. Multiple impellers are often used in industrial applications to increase the efficiency of mixing in an agitated tank because the ratio between liquid height and tank diameter is usually larger than unity. The design and scale-up of these reactors generally depend on the quantification of the hydrodynamics and transport characteristics of the system that are mainly dependent on the way dispersed phase is dispersed throughout the tank [8]. In literature, the hydrodynamics of transport characteristic in stirred tank are successfully predicted using CFD. It is an effective tool in modelling of fluid related systems. In this technique, various multiphase models are available, however, in literature, Eulerian-Eulerian model is the most successfully and commonly used model without incorporating the distributions of bubbles [5], [6], [9]-[11]. In this study, double Rushton impeller is being studied in gas-liquid phase taking constant bubble diameter with Eulerian-Eulerian multiphase model. This study predicts local gas hold up, local interfacial area and mass transfer and compared with published literature.

T.T. Devi is with National Institute of Technology, Langol-795004, Manipur, India (corresponding author; phone: +91-385-2058566; fax: +91-385-2413031; e-mail: thiyam85@gmail.com).

B. Kumar is with Indian Institute of Technology, Guwahati-781039, Assam, India (e-mail: bimk@iitg.ernet.in).

II. NUMERICAL MODEL

The details of numerical equations and techniques involved in CFD simulation will be presented in this section.

A. Governing Equations

Eulerian-Eulerian multiphase model is used to simulate the hydrodynamics of flow in this study. The phases (continuous and disperse) are treated as interpenetrating media identified by their local volume fractions. The volume fractions sum to unity and are calculated by using continuity equation. The Reynolds averaged mass and momentum balance equations are solved for each of the phases and are given as follows:

Continuity equation:

$$\frac{\partial}{\partial t}(\alpha_i \rho_i) + \nabla \cdot (\alpha_i \rho_i \vec{U}_i) = 0 \quad (1)$$

$$\alpha_l + \alpha_g = 1 \quad (2)$$

where, ρ_i , α_i and \vec{U}_i are density, volume fraction and mean velocity, respectively, of phase i (l or g).

Momentum equation:

$$\frac{\partial}{\partial t}(\alpha_i \rho_i \vec{U}_i) + \nabla \cdot (\alpha_i \rho_i \vec{U}_i \vec{U}_i) = -\alpha_i \nabla p + \nabla \cdot \bar{\tau}_{\text{eff}} + \vec{R}_i + \vec{F}_i + \alpha_i \rho_i \vec{g} \quad (3)$$

where, p is the pressure shared by the two phases and \vec{R}_i is the inter-phase momentum exchange terms. \vec{F}_i , represents the Coriolis and centrifugal forces applies in MRF (multiple reference frame) impeller model which is used in this study as impeller model.

$$\vec{F} = -2\alpha_i \rho_i \vec{N} \times \vec{U}_i - \alpha_i \rho_i \vec{N} \times (\vec{N} \times \vec{r}) \quad (4)$$

where, \vec{N}_i is angular velocity (rad s^{-1}) and \vec{r} is position vector (m).

The Reynolds stress tensor $\bar{\tau}_{\text{eff}}$ is the laminar and turbulent stresses and by Boussinesq hypothesis, it is given as

$$\bar{\tau}_{\text{eff}} = \alpha_i (\mu_{\text{lam},i} + \mu_{t,i}) (\nabla \vec{U}_i + \nabla \vec{U}_i^T) - \frac{2}{3} \alpha_i (\rho_i k_i + (\mu_{\text{lam},i} + \mu_{t,i}) \nabla \cdot \vec{U}_i) \vec{I} \quad (5)$$

$\mu_{lam,i}$ and $\mu_{t,i}$ are laminar and turbulent viscosity for phase i . k_i is turbulent kinetic energy for phase i and \bar{I} is unit tensor.

B. Turbulence Model Equations

Standard $k-\varepsilon$ turbulence model is adequate for many engineering applications [12] and is used in this study with dispersed $k-\varepsilon$ multiphase turbulence model to simulate the gas-liquid phase flow as gas (secondary phase) is dispersed in continuous liquid (primary phase). The governing equations of turbulent kinetic energy, k and turbulent dissipation rate, ε , are solved only for liquid phase as

$$\frac{\partial}{\partial t}(\rho_l \alpha_l k_l) + \nabla \cdot (\rho_l \alpha_l \bar{U}_l k_l) = \nabla \cdot \left(\alpha_l \frac{\mu_{t,l}}{\sigma_k} \nabla k_l \right) + \alpha_l G_{kl} - \rho_l \alpha_l \varepsilon_l + \rho_l \alpha_l \Pi_{kl} \quad (6)$$

$$\frac{\partial}{\partial t}(\rho_l \alpha_l \varepsilon_l) + \nabla \cdot (\rho_l \alpha_l \bar{U}_l \varepsilon_l) = \nabla \cdot \left(\alpha_l \frac{\mu_{t,l}}{\sigma_\varepsilon} \nabla \varepsilon_l \right) + \alpha_l \frac{\varepsilon_l}{k_l} (C_{1\varepsilon} G_{kl} - C_{2\varepsilon} \rho_l \varepsilon_l) + \rho_l \alpha_l \Pi_{\varepsilon l} \quad (7)$$

Turbulent liquid viscosity is given as

$$\mu_{t,l} = \rho_l C_\mu \frac{k_l^2}{\varepsilon_l} \quad (8)$$

G_{kl} is the rate of production of turbulent kinetic energy. Π_{kl} and $\Pi_{\varepsilon l}$ represent the influence of the dispersed phase on the continuous phase [13]. C_μ , $C_{1\varepsilon}$, $C_{2\varepsilon}$, $C_{3\varepsilon}$, σ_k and σ_ε are constants of standard $k-\varepsilon$ model. Their values are 0.09, 1.44, 1.92, 1.2, 1.0 and 1.3 respectively.

C. Inter-Phase Momentum Exchange

Inter-phase force comprises of lift force, virtual force and drag force. Drag force is the most important inter-phase force acting on the bubbles resulting from the mean relative velocity between the two phases and an additional contribution resulting from turbulent fluctuations in the volume fraction due to averaging of momentum equations [14]. In this study, only drag force is considered as in many studies it has been neglected because of its less significance in phase interaction [8], [10], [15]. Hence, \bar{R}_i from (3) reduced only to drag force as

$$\bar{R}_i = -\bar{R}_g = K(\bar{U}_g - \bar{U}_l) \quad (9)$$

K is the liquid-gas exchange co-efficient given as

$$K = \frac{3}{4} \rho_l \alpha_l \alpha_g \frac{C_D}{d_b} |\bar{U}_g - \bar{U}_l| \quad (10)$$

d_b is the bubble diameter and C_D is the drag co-efficient defined as function of relative Reynolds number, Re_p :

$$Re_p = \frac{\rho_l |\bar{U}_g - \bar{U}_l| d}{\mu_l} \quad (11)$$

Drag co-efficient is calculated using standard correlation of [16] which is written as

$$C_D = \begin{cases} \frac{24(1 + 0.15 Re_p^{0.687})}{Re_p} \\ \end{cases} \quad (12)$$

for $Re_p \leq 1000.0$ or 0.44 for $Re_p > 1000.0$. This correlation is applied for still water which is not realistic because bubble moves in turbulent flows; hence a modified drag force was used by [17] considering the effects of turbulence. It is based on a modified viscosity term in the relative Reynolds number [1] and is given as

$$Re_p = \frac{\rho_l |\bar{U}_g - \bar{U}_l| d}{\mu_l + C \mu_{t,l}} \quad (13)$$

C is set to 0.3 by [17].

D. Mass Transfer Model

Mass transfer co-efficient, k_L , suggested by [18], [19] based on [20] theory of isotropic turbulence is given as

$$k_L = K D_l^{0.5} \left(\frac{\varepsilon_l}{\nu_l} \right)^{0.25} \quad (14)$$

where, D_l is the diffusion co-efficient and ε_l is the turbulent dissipation rate in the liquid phase; ν_l is the liquid dynamic viscosity and $K=0.4$ is model constants. And volumetric mass transfer co-efficient is given as

$$k_L a = K D_l^{0.5} \left(\frac{\varepsilon_l}{\nu_l} \right)^{0.25} a \quad (15)$$

a is interfacial specific area and is a function of local gas volume fraction and bubble diameter; given as

$$a = \frac{6\alpha_g}{d_b} \quad (16)$$

E. Numerical Techniques

Fluent 6.3 is used in this study. MRF impeller model with pressure based implicit steady solver is used. First order differencing discretization scheme is used to solve the equations of flow, volume fraction and turbulence. Solution is considered as converged when the volume fraction has no

significant changes after certain iterations and is achieved when residuals fell nearly below 10^{-3} .

III. SOLUTION DOMAIN AND BOUNDARY CONDITIONS

The tank geometry and generated grid (unstructured) is shown in Fig. 1. Double Rushton impeller (diameter, $d=0.0973$) is provided at clear off distances of 0.146 m and 0.438 m from the tank bottom. Stirred tank ($T=0.292$) is filled with water up to the height of 0.584 m. Impeller is rotated at 450 rpm speed. Gas is supplied at the rate of $1.67 \times 10^{-4} \text{ m}^3/\text{s}$ through ring sparger which is kept below the impeller as an inlet boundary condition. Gas volume fraction of 1 is provided at sparger inlet. Diameter of bubble is taken as 0.0023m. No slip conditions are applied at all the walls and shaft. Symmetry condition at free surface is used in the simulation.

Single impeller of Rushton and CD-6 impeller is used for the simulation of mass transfer co-efficient and Table I shows its geometrical detail.

TABLE I
 GEOMETRICAL DIMENSIONS OF SINGLE RUSHTON AND CD-6 IMPELLER

Impeller	T (m)	D (m)	Speed, N (rpm)	Gas flow rate, v_g (m/s)	Bubble diameter, d_b (mm)
Rushton	0.63	0.21	390	0.0074	5.3
CD-6	0.63	0.21	390	0.0074	5.3

IV. RESULT AND DISCUSSION

The simulated gas-liquid velocity, its gas hold up, specific area and mass transfer co-efficient comparing with other published literature will be presented in this section.

A. Flow Pattern in Gas-Liquid Flow

The performance and designing of stirred tank reactors directly relates with the efficiency in mixing which is defined by hydrodynamics (flow velocity) and mass transfer characteristics (volumetric mass transfer rate, gas hold up, specific area, etc.). The vectors of mean velocity for water and gas are shown in Fig. 2. The magnitude of velocity is higher at the impeller discharge region in water and gas phase, however, gas velocity is observed significantly higher from the water velocity. There is no effect of sparger is observed in velocity, it is apparently due to small diameter of sparger, even though, the design of sparger is not objective of this study.

B. Local Gas Hold Up

Gas hold up is fundamental parameter in describing the mixing behavior, fluid dynamics and oxygen mass transfer characteristics of aerated vessels and the gas-liquid volumetric mass transfer coefficient (KLa) depends on gas hold-up in gas sparged, non-agitated fermenter [21]. As such, it is crucial in the proper design and scale-up of in aerobic fermentation processes.

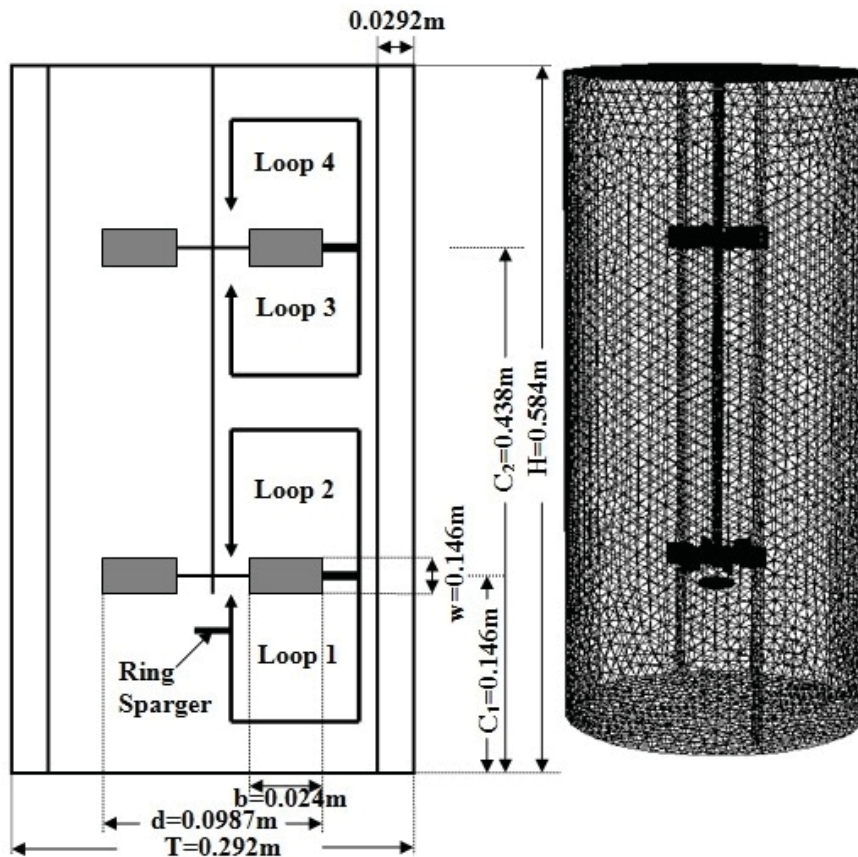


Fig. 1 Solution Domain (tank geometry) and mesh generated for double impeller

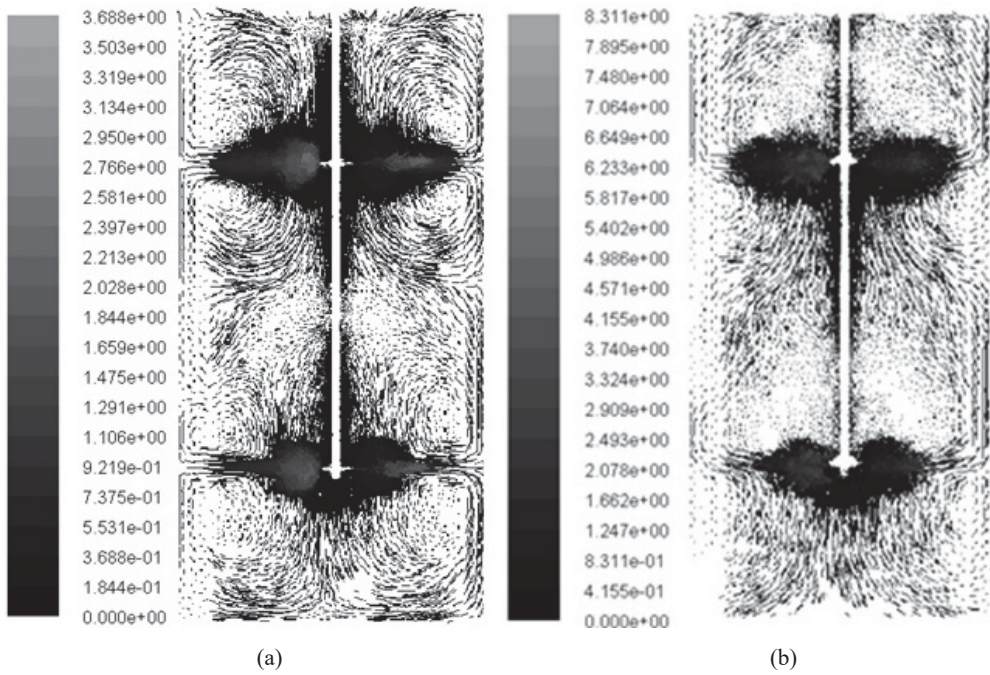


Fig. 2 Vectors of mean velocity (m/s) for (a) water and (b) gas

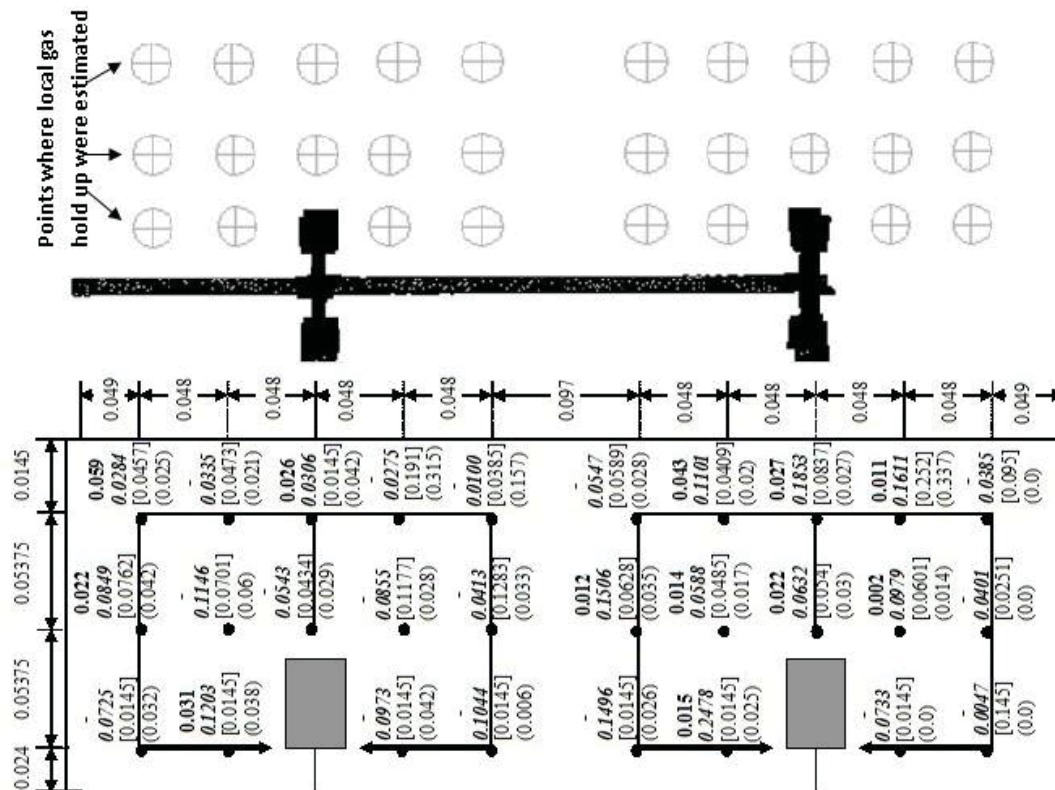
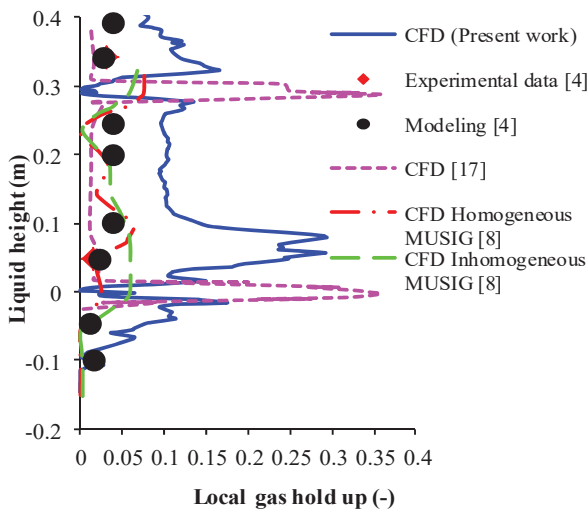
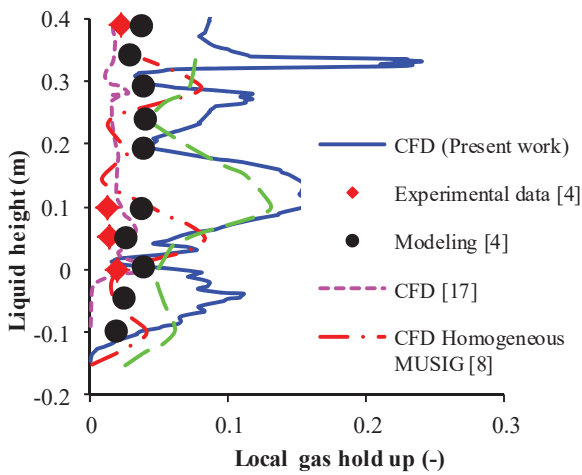


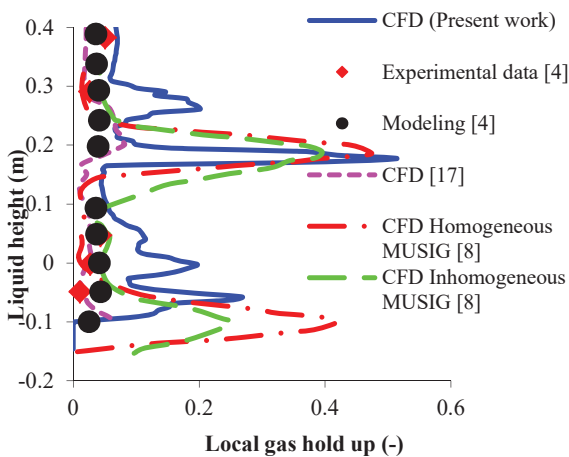
Fig. 3 Comparison of local gas hold up between experimental data of Alves et al. [4] (bold) and CFD present work (italics), Ranganathan & Sivaraman [8] CFD model Inhomogeneous [] and Homogeneous ()



(a)



(b)



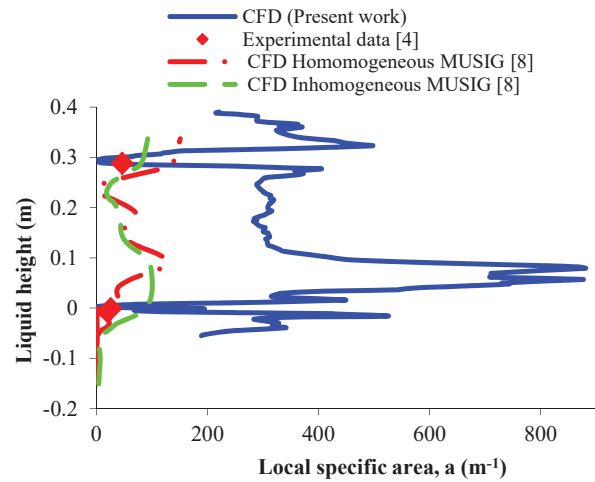
(c)

Fig. 4 Axial variation of local gas hold up at different radial positions, (a) $r=0.024\text{m}$ (b) $r=0.07775\text{m}$ and (c) $r=0.1315\text{m}$

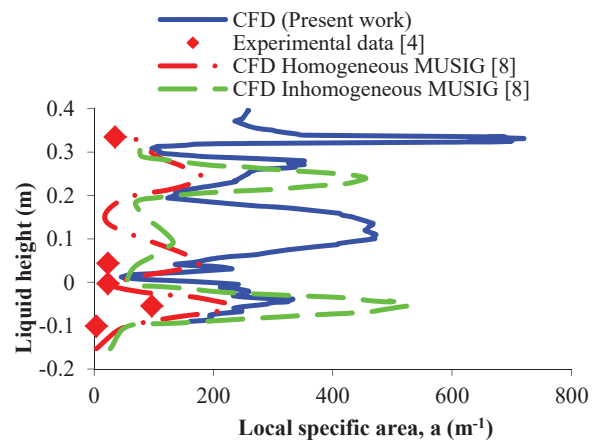
The comparisons of simulated local gas hold-up with experimental results measured at various locations are presented in Fig. 3. The predicted point wise gas hold-up at different spatial point (Fig. 3) is under-predicted at near the impeller region and over-predicted outside impeller region but it is in reasonable agreement with other simulated results and is close to the results of [8] Inhomogeneous model. In Figs. 4 (a)-(c); gas hold-up is observed higher at both the impeller region in all the simulated results of present study and published literature. The magnitude of gas hold-up is predicted higher at the upper impeller tip than the lower impeller. The predicted result is under-predicted from the experimental result; however, it is reasonable agreement with other simulated results.

C. Local Specific Area

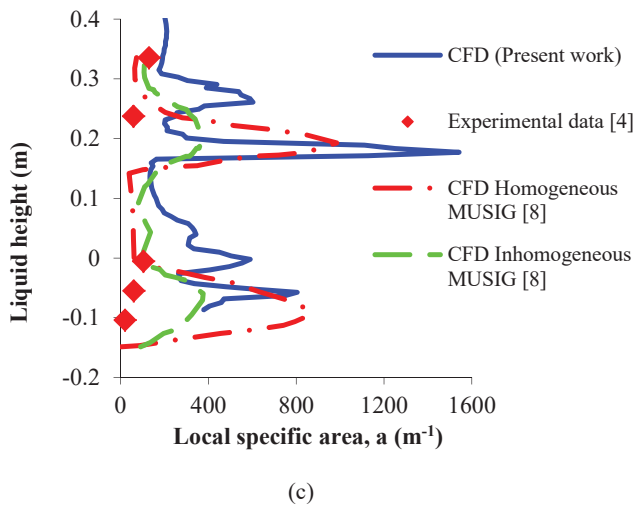
Interfacial specific area of gas is an important parameter to be analyzed for understanding the interfacial phenomena between gas-liquid phases and its comparison of predicted results with experimental and other simulated published literature at different radial distance is shown in Figs. 5 (a)-(c).



(a)



(b)



In Fig. 5, predicted local specific area is observed higher at impeller region and over-predicted from the experimental results, however, it is close to the simulated results of homogeneous model of [8].

Fig. 5 Comparison of predicted local specific area, a (m^{-1}) with experimental and simulated results of published literature at different radial positions (a) $r=0.024m$ (b) $r=0.07775m$ and (c) $r=0.1315m$

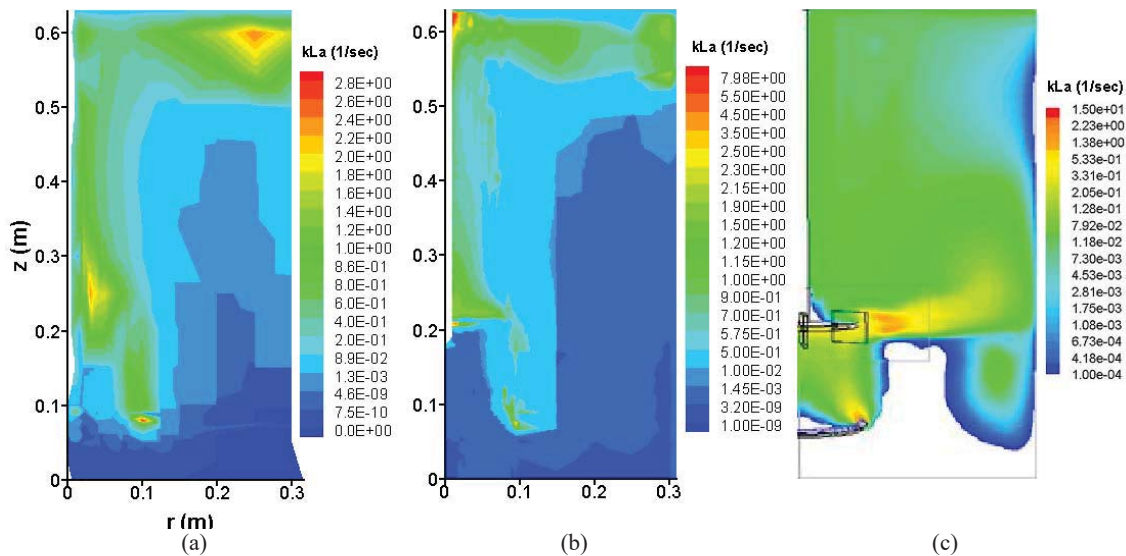


Fig. 6 Comparison of volumetric mass transfer co-efficient (K_{La}) of (a) Rushton and (b) CD-6 impeller at 3 secs of gas flow rate $0.0074m/s$ with (c) [23] simulated result of Rushton impeller

D. Mass Transfer Coefficient (K_{La})

The volumetric mass transfer coefficient is the most influential multiphase characteristic in gas-liquid phase for the better performance of any system. The mass transfer produced by different types of impeller is an important parameter to be understood. Most studies were performed on standard impeller like Rushton impeller which has straight blade and its multiphase characteristics are well known, however, other type of impeller like concave blade like CD-6 impeller which is adopted in this study does not have enough studies and hence, its multiphase characteristics are always unknown. But fortunately, some few studies were carried out on the study of CD-6 impeller by [22] and [23]. Due to the variation in the impeller type in its shape particularly, the multiphase characteristic including mass transfer also significantly varies

and such type of studies were performed by [23] on Rushton and CD-6 impeller. The comparison of volumetric mass transfer coefficient of Rushton and CD-6 impeller is presented in Fig. 6. This particular simulation was performed on unsteady time step to understand the variation of mass transfer with time where air is continuously supplied through sparger. Volumetric mass transfer co-efficient of CD-6 impeller is observed higher than the Rushton impeller which is similar to the results of [23] and [22]. This is because of the fact that due to the concave nature of CD-6 impeller pumps the fluid slightly downward around the impeller discharge region while Rushton impeller pumps slightly upward leading to the poor circulation of fluids in the lower region. The mass transfer in both cases is observed higher near the impeller discharge region upwards to the central part of impeller where the shaft is mounted, at the sparger inlet and on the free surface. This is

obvious thing that due to continuous rotation of impeller, its discharge region with its sweep region gets proper circulation of fluids and due to the formation of vortex, the upward central part is exposed to atmosphere allowing air to mix with water and on the free surface, the outer layer of fluid is also exposed to the atmosphere which increases the tendency of fluid circulation. The comparison of mass transfer with [23] result observed some discrepancies this because in the present study the mass transfer is measured at the initial 3 secs time under unsteady condition while in [23], it performed under steady condition measured at fully developed turbulent regime.

V. CONCLUSION

The characteristics of multiphase in terms of gas hold up, interfacial specific area and mass transfer is predicted at different axial and radial positions. These results were compared with experimental results of published literature. Results were found over-predicted from the experimental results; however, it is in reasonable agreement with other simulated published literature. The mass transfer co-efficient of CD-6 impeller is observed higher than the Rushton impeller.

REFERENCES

- [1] Bakker and H.E.A. Van den Akker. "A computational model for the gas-liquid flow in stirred reactors," *Chem. Eng. Res. Des.*, Vol. 72, pp. 594-606, 1994.
- [2] L. Lane, M. P. Schwarz, and G. M. Evans. "Predicting gas-liquid flow in a mechanically stirred tank," *Appl. Math. Model.*, vol. 2, pp. 223-235, 2002.
- [3] L. Lane, M. P. Schwarz, and G. M. Evans. "Numerical modelling of gas-liquid flow in stirred tanks," *Chem. Eng. Sci.*, vol. 60, pp. 2203-2214, 2005.
- [4] S. S. Alves, C. I. Mania and J. M. T. Vasconcelos. "Experimental and modeling of gas dispersion in double turbine stirred tank", *Chem. Eng. Sci.*, vol. 89, pp 109-117, 2002a.
- [5] N. G. Deen, T. Solberg and B. H. Hjertager. "Flow generated by an aerated Rushton impeller: two phase PIV experiments and numerical simulations," *Canadian J. Chem. Eng.*, Vol. 80, pp. 638-652, 2002.
- [6] A. R. Khopkar and V. V. Ranade. "CFD simulation of gas-liquid vessel: VC, S33 and L33 flow regimes," *AIChEJ*, vol. 52(5), pp. 1654-1672, 2006.
- [7] G. Montante, A. Paglianti, and F. Magelli. "Experiments and simulations of gas-liquid stirred vessels," in *Proc. of 12th European Conf. on Mixing*, Bologna, 2006, pp. 137-144.
- [8] P. Ranganathan. and S. Sivaraman. "Investigations on hydrodynamics and mass transfer in gas-liquid stirred reactor using computational fluid dynamics," *Chem. Eng. Sci.*, vol. 66, pp. 3108-3124, 2011.
- [9] G. L. Lane, M. P. Schwarz, and G. M. Evans. "Numerical modelling of gas-liquid flow in stirred tanks," *Chem. Eng. Sci.*, vol. 60, pp. 2203-2214, 2004.
- [10] J. C. Scargiali, F. D'Orazio, F. Grisafi, and A. Brucato. "Modelling and simulation of gas-liquid hydrodynamics in mechanically stirred tanks," *Chem. Eng. Res. Des.*, vol. 85, pp. 637-646, 2007.
- [11] G. Montante, A. Paglianti and F. Magelli. "Experimental analysis and computational modelling of gas-liquid stirred vessels," *Chem. Eng. Res. Des.*, vol. 85(A5), pp. 647-653, 2007.
- [12] V. V. Ranade. "Computational flow modelling for chemical reactor engineering," Academic press, New York, 2002.
- [13] S. E. Elgobashi, and M. A. Rizk. "A two-equation turbulence model for dispersed dilute confined two-phase flows," *Inter. J. Multiphase Flow*, vol. 15(1), pp. 119-133, 1999.
- [14] Fluent 6.2 & 6.3 User's Guide, 2005 & 2006.
- [15] A. R. Khopkar, A. R. Ramamohan, V. V. Ranade, and M. P. Dudukovic. "Gas-liquid flow generated by a Rushton turbine in stirred vessel: CART/CT measurements and CFD simulations," *Chem. Eng. Sci.*, vol. 60, pp. 2215-2229, 2005.
- [16] M. Ishii, N. Zuber. Drag coefficient and relative velocity in bubbly, droplet or particulate flows," *AIChE J.*, vol. 25, pp. 843-855, 1979.
- [17] F. Kerdouss, A. Bannari, and P. Proulx. "CFD modeling of gas dispersion and bubble size in a double turbine stirred tank," *Chem. Eng. Sci.*, vol. 61, pp. 3313-3322, 2006.
- [18] P. V. Danckwerts. "Significance of liquid-film coefficients in gas absorption," *Ind. Eng. Chem.*, vol. 43, pp. 1460-1467, 1951.
- [19] J. C. Lamont and D. S. Scott. "An eddy cell model of mass transfer into the surface of a turbulent liquid," *AIChE J.*, vol. 16, pp. 513-519, 1970.
- [20] Kolmogorov, A.N. The local structure of turbulence in incompressible viscous fluid for very large Reynolds numbers, *Doklady Akademii Nauk SSSR*, Vo. 30, pp. 301-305, 1941.
- [21] W. J. McManamey and D. A. Wase. "Relationship between volumetric mass transfer coefficient and gas hold up in airlift fermenters," *Biotechnol. Bioengg.*, vol. 28, pp. 1446-1448, 1986.
- [22] K. J. Myers, A. J. Thomas, A. Bakker, and M. F. Reeder. "Performance of gas dispersion impeller with vertically asymmetric blades," *Chem. Eng. Res. Des.*, vol. 77, pp. 728-730, 1999.
- [23] J. Gimbut, C. D. Rielly, and Z. K. Nagy. "Modelling of mass transfer in gas-liquid stirred tanks agitated by Rushton turbine and CD-6 impeller: A scale-up study," *Chem. Eng. Res. Des.* Vol. 87, pp. 437-451, 2009.